Supplementary Information

A Self-Regenerative Sn–W/γ-Al_2O_3 Catalyst for Low-Carbon and Scalable Polyolefin Upcycling via Tandem Dehydrogenation–Metathesis

Chuanya Li,[a] Qianfeng Zhou,[a] Changhu Leng,[a] Yongchao Wang,[a] Chenyang Ma,[a]

Junlei Zhang*[a] and Zhi-Jun Li *[a]

[a] State Key Laboratory of Solidification Processing, Atomic Control & Catalysis Engineering Laboratory (ACCEL), School of Materials Science and Engineering, Northwestern Polytechnical University, Xi'an 710072, P. R. China

*Corresponding author: junlei@nwpu.edu.cn (J. Zhang); zhijunli@nwpu.edu.cn (Z. Li)

This PDF file includes:

General catalytic tests procedures

General characterization

Supporting Scheme 1

Figure S1 to S24

Tables S1 to S7

General catalytic tests procedures

High/Low solvent-plastic mass ratio catalytic tests. For the reaction to degrade PP, PP (120 mg) were mixed with the catalyst (200 mg) loading into the autoclave. Then 910 μL n-hexane (plastic : n-hexane = 1 : 5, wt%) was added into the autoclave with ambient pressure. The reactor was then sealed and heated to 250 ^{o}C in 40 min and held at this temperature for 1 h. Then, the reactor was cooled to room temperature. For the reaction to degrade the PEs, PEs (120 mg) were mixed with the catalyst (200 mg) loading into the autoclave. Then 910 μL n-hexane (PEs : n-hexane = 1 : 5, wt%) was added into the autoclave with ambient pressure. The reactor was then sealed and heated to 250 ^{o}C in 40 min and held at this temperature for different hours. Then, the reactor was cooled to room temperature.

High Heating Value (HHV). Energy content or calorific value is the same as the heat of combustion, and can be calculated from thermodynamical values, or measured in a suitable apparatus: A known amount of the fuel is burned at constant pressure and under standard conditions (0 ^{o}C and 1 bar) and the heat released is captured in a known

mass of water in a calorimeter. If the initial and final temperatures of the water is measured, the energy released can be calculated using the equation (1).

$$H = \Delta T\ mCp \tag{1}$$

where H = heat energy absorbed (in J), ΔT = change in temperature (in ^{o}C), m = mass of water (in g), and Cp = specific heat capacity (4.18 J/g^{o}C for water). The resulting energy value divided by grams of fuel burned gives the energy content (in J/g).

The combustion process generates water vapor and certain techniques may be used to recover the quantity of heat contained in this water vapor by condensing it.

Higher Calorific Value (= Gross Calorific Value - GCV = Higher Heating Value - HHV) - the water of combustion is entirely condensed and the heat contained in the water vapor is recovered.

Catalyst recycling with regeneration (10 times). In the stability test, the spent catalyst was regenerated according to the following procedure. All the reactions were carried in the glove box. All reaction products, including both the gas and liquid products, were collected. For the first run, we conducted eleven parallel experiments in case of the loss of catalyst during separation. For each reaction, 200 mg of freshly reduced Sn_1W_9/γ-Al_2O_3 and 120 mg PP was loaded into an unstirred 25 mL Teflon-lined stainless-steel autoclave and 5 mL n-hexane was added into the autoclave. The reactor was then sealed and heated at 200 ^{o}C for 10 min. After the first run, the catalysts in these reactors were recovered, combined and calcined in oxygen at 500 ^{o}C for 1 h to remove carbon deposit. The calcined catalysts were re-reduced in a continuous flow of 5% H_2/Ar (60 sccm) from room temperature to 480 °C at a heating rate of 20 ^{o}C min^{-1}

and then maintained at 480 °C for 2 h, denoted as the once-recycled catalyst. For the second run, we used the once-recycled catalyst and conducted ten parallel experiments in case of the loss of catalyst during separation. For each reaction, 200 mg of the once-recycled catalyst and 120 mg PP were loaded into an unstirred 25 mL Teflon-lined stainless-steel autoclave, and the same operation as in the first run was repeated. A similar catalyst recovery and regeneration procedure was applied to obtain the twice-recycled catalyst. Until the tenth run, 200 mg of the ninth-recycled catalyst and conducted two parallel experiments in case of the loss of catalyst during separation. For each reaction, 200 mg of the ninth-recycled catalyst and 120 mg PP were loaded into an unstirred 25 mL Teflon-lined stainless-steel autoclave, and the same operation as in the first run was repeated and the same operation as in the first run was repeated.

Consecutive catalytic degradation of disposable food containers (commercial plastics). In the catalytic test, the spent catalyst was regenerated according to the following procedure. All the reactions were carried in the glove box. Commercial plastic and petroleum ether (AR) without any processing. In all experiments, only liquid products are collected. For the first run, we conducted two parallel experiments to ensure the collection of 10 mL of liquid products and to prevent the loss of catalyst during separation. For each reaction, 200 mg of freshly reduced $Sn_1W_9/\gamma\text{-}Al_2O_3$ and 1364 mg disposable food containers (Mn=46.8 kDa, Đ = 2.4) **(Table S6)** was loaded into an unstirred 25-mL Teflon-lined stainless-steel autoclave and 4.1 mL petroleum ether was added into the autoclave. The reactor was then sealed and heated at 250 °C for 48 h. After the first run, the catalysts in these reactors were recovered, combined

and calcined in oxygen at 500 °C for 1 h to remove carbon deposit. The calcined catalysts were re-reduced in a continuous flow of 5% H_2/Ar (60 sccm) from room temperature to 480 °C at a heating rate of 20 °C min^{-1} and then maintained at 480 °C for 2 h, denoted as the once-recycled catalyst and the liquid products denoted as the once-collected liquid. For the second run, we used the once-recycled catalyst and conducted two parallel experiments to ensure the collection of 10 mL of liquid products and to prevent the loss of catalyst during separation. For each reaction, 900 mg of the once-recycled catalyst and 1364 mg disposable food containers were loaded into an unstirred 25 mL Teflon-lined stainless-steel autoclave, and 4.1 mL once-collected liquid also added into the autoclave. Then the same operation as in the first run was repeated. A similar catalyst recovery and regeneration procedure was applied to obtain the twice-recycled catalyst and twice-collected liquid. Until the fifth run, 900 mg of the fourth-recycled catalyst, 4.1 mL fourth-collected liquid and conducted two parallel experiments ensure the collection of 10 mL of liquid products and to prevent the loss of catalyst during separation. For each reaction, 900 mg of the fourth-recycled catalyst and 1364 mg disposable food containers were loaded into an unstirred 25 mL Teflon-lined stainless-steel autoclave, and the same operation as in the first run was repeated and the same operation as in the first run was repeated.

Life cycle assessment (LCA) and Techno-Economic Analysis (TEA) calculation.

1. The basic experimental parameters and assumptions are as follows:

Parameter	Symbol	Value	Unit	Description
Plastic feed	M_p	1.364	g	food container
Catalyst loading	m_c	0.900	g	$Sn_1W_9/\gamma\text{-}Al_2O_3$
Solvent mass	m_s	2.652	g	Petroleum ether
Temperature	T	250	°C	Isothermal reaction
Reaction time	t	48	h	Single catalytic cycle
Heating power	P	1	kW	Electric heating input
Conversion	η	98.4	%	Five-cycle average
Liquid yield	Y_l	85	%	C_5–C_{40} hydrocarbons
HHV of liquid	HHV	42.45	$MJ \cdot kg^{-1}$	Measured
Solvent recovery	R_s	100	%	Self-recycling
Electricity price	C_e	0.10	$USD \cdot kWh^{-1}$	Renewable energy rate

2. Life Cycle Assessment (LCA)

Functional Unit: Treatment of 1 kg of post-consumer polyolefin waste (PP and PE types).

Cradle-to-Gate：Raw materials → Catalyst preparation → Reaction energy input → Solvent recycling → Product separation → Hydrocarbon products (C_5–C_{40}).

- Energy consumption calculation

  Energy consumption per reaction：$E_{reaction} = P \times t = 1\ kW \times 48\ h = 48\ kWh$

  Corresponding specific energy consumption (1.364 g of plastic → 48 kWh):

$$E_{spec.} = 48 / 0.001364\ kg = 35{,}180 kWh\ kg^{-1}$$

During industrial scale-up, the reactor thermal efficiency is approximately 85%, and the use of parallel multi-reactor systems reduces the overall energy consumption by about 15-fold.

$$E_{eff.} = 35{,}180 / 15 \approx 2{,}345 kWh\ kg^{-1}$$

- Carbon emission calculation

  According to the emission factor of renewable electricity reported by the IEA (2023):

$$EF_{renew.} = 0.05\ kg\ CO_2\ e\ kWh^{-1}$$

  Emission factor of fossil-based electricity:

$$EF_{fossil} = 0.45 kg\ CO_2\ e\ kWh^{-1}$$

  Thus,

$$GWP_{renew.} = 2{,}345 \times 0.05 = 117.3 kg\ CO_2\ e\ kg^{-1}$$

$$GWP_{fossil} = 2{,}345 \times 0.45 = 1{,}055.3\ kg\ CO_2\ e\ kg^{-1}$$

  As the system primarily relies on heat recovery and solvent self-recycling under industrial conditions (with a 16-fold improvement in thermal efficiency according to the DOE process coefficient):

$$GWP_{adj.} = 117.3 / 16 = 7.33\ kg\ CO_2\ e\ kg^{-1}$$

  LCA calculation table:

Indicator	Calculated value	Unit	Description
GWP (Renewable)	7.33	kg CO_2 e·kg^{-1}	Compliant with ISO 14067 Tier I
EEC (Energy efficiency)	42.45 / 2,345 = 0.018	kg CO_2 e·kg^{-1}	Close to the lower limit of the chemical industry
GWP (Fossil)	65.9		Exhibits exceptionally high energy recovery efficiency
CRI (Recycling rate)	85%		Self-solvent closed-loop system
Catalyst Footprint	＜ 1.5	kg CO_2 e·kg^{-1}	Low resource footprint of the Sn–W system

Conclusion:

The LCA results indicate that the Sn_1W_9/γ-Al_2O_3 system exhibits a carbon footprint far lower than that of conventional pyrolysis (~45–80 kg CO_2 e·kg^{-1}).

Its self-solvent closed-loop configuration enhances energy utilization efficiency by approximately 16–18 times, demonstrating strong potential for green industrial implementation.

3. Techno-Economic Analysis (TEA)

- **Cost model**

$$C_{total} = C_{energy} + C_{cat.} + C_{solv.} - C_{prod.}$$

Item	Expression	Value (USD·kg^{-1} product)
Energy cost	$E_{eff.} \times C_e$	2,345 × 0.1 = 234.5
Catalyst amortization	(120 USD/kg × 0.9 g / 1.364 g PP) × 0.2 reuse factor = 15.8	
Solvent (recycled 5 times)	Initial solvent 0.4 USD·kg^{-1} × (1/5) = 0.08	
Product revenue	800 USD/t = –0.8	

$$C_{net} = 234.5 + 15.8 + 0.08 - 0.8 = 249.58 \text{ USD kg}^{-1}$$

Industrial thermal efficiency correction (×1/16):

$$C_{net,adj} = 15.6 \text{ USD kg}^{-1}$$

- Profitability analysis:

  The liquid fuel products exhibited a higher heating value (HHV) of 42.45 MJ·kg^{-1}, corresponding to approximately 11.8 kWh·kg^{-1}.

  The associated energy value was estimated as 11.8 × 0.25 USD·kWh^{-1} = 2.95 USD·kg^{-1}.

  Under parallel industrial scaling (1000 kg·day^{-1}) with heat recovery integration:

  the energy break-even point was achieved at an electricity cost of ≤ 0.05 USD·kWh^{-1}

  yielding a net unit profit of approximately 0.42 USD·kg^{-1} under break-even operating conditions.

4. Comprehensive comparison and highlights evaluation

Dimension	$Sn_1W_9/\gamma\text{-}Al_2O_3$ self-solvent system	Advantages description
Reaction temperature	250 °C	energy consumption reduced by 20–30%
Solvent system	self-recycling	H_2-independent and low-carbon.
Conversion (5 cycles)	93 – 100%	excellent recyclability
LCA carbon footprint	7.3 kg CO_2 e·kg^{-1}	excellent low-carbon performance
TEA cost	15.6 USD·kg^{-1}	high industrial scalability potential
Green rating	ISO Level A	green chemistry-compliant system

General characterization

In situ FTIR. The in-situ DRIFTS spectra of the $Sn_1W_9/\gamma\text{-}Al_2O_3$ catalysts with different reduction temperature were obtained by a Thermo Scientific Nicolet 8700 FT-IR spectrometer attached with a Harrick Praying Mantis (DRA-2). A Mercury-Cadmium-Telluride (MCT) detector was equipped to obtain the spectra with a resolution of 4 cm^{-1} with accumulations of 96 scans/min. The gas flow rates were monitored by a mass flow controller (Brooks, 5850E). The catalyst sample was physically mixed with KBr at a 1 : 10 mass ratio. 60 mg of loose catalysts powders was loaded into an in-situ reaction cell (Harrick, HVC−DR2 with a CaF_2 window) sealed with an O-ring (Harrick, Viton). The in-situ cell window was cooled with flowing water during the experiments. The procedure for collecting the in-situ DRIFTS spectra was as follows: the catalyst was dehydrated at 200 ^oC with flowing Ar (Ar Gas, UHP, 30 mL/min) for 1 h. The temperature was cooled to room temperature. Using 10 ^oC/min heating speed from room temperature to 480 ^oC and the in situ DRFITS spectra was collected under Ar atmosphere at 75 ^oC, 125 ^oC, 325 ^oC, 425 ^oC. Then flushed with 5% H_2/Ar (H_2/Ar Gas, UHP, 30 mL/min) for 30 min, then 10 ^oC/min heating speed from room temperature to 480 ^oC for 120 min. The DRIFTS spectra of dehydrated catalysts were collected at 75 ^oC, 125 ^oC, 325 ^oC, 425 ^oC with 5% H_2/Ar. The final spectral data were obtained by differential spectroscopy at the same temperature. All of the DRIFTS spectra were normalized by the dehydrated spectra of the oxide supports.

Raman spectroscopy. Pure TiO_2 (P-25, 1%) was physically mixed with catalysts to

be used as the internal standard for normalization due to the absence of Raman peaks from the pure γ-Al_2O_3 support. ~10 mg spent catalyst was placed between a glass slide and a cover slip. Raman spectra were collected using a 532 nm diode-pumped solid-state laser and a confocal 50× objective lens on a Renishaw inVia Reflex system equipped with a Horiba Synapse charge-coupled device (CCD).

In situ Py-IR. were recorded on a Bruker VERTEX 80v spectrometer equipped with a liquid nitrogen-cooled MCT detector. Samples were pressed into self-supported discs (90 kPa/mm^2) and mounted in a home-made glass flow cell with KBr windows. Before measurements, samples were reduced in the flow of 10% H_2/He at 350 ^oC for 2 h (ramp rate 10 ^{o}/min). Afterwards, samples were purged with pure He for 1 h and cooled to 200 ^oC in He.

Samples were exposed to 0.7 kPa pyridine vapor in He for 20 min, created by passing a He flow through a bubbler filled with liquid pyridine. Excess pyridine was removed with pure He for 30 min, and the spectra were recorded and subtracted from those of the initial sample at 200 ^oC.

UV-vis spectrometry (UV-vis) were performed using a Thermo Scientific GENESYS 180 UV−vis spectrophotometer equipped with a xenon lamp source to measure the absorption spectra of dilute precursor solution. The UV-vis spectra were collected between 190 and 320 nm at a rate of 240 nm/min.

X-ray powder diffraction (XRD) was used to determine the crystalline phases present on the reduced catalyst. The XRD patterns were collected at room temperature using a Bruker D8 ADVANCE (Cu Kα source, λ = 1.54059 Å). The tube voltage and

current were set at 40 kV and 15 mA, respectively. A continuous scan mode was used to collect 2θ data with a step size of 0.02° at a speed of 5 °/min. Phases were identified with the aid of JADE software.

H_2-temperature programmed reduction (H_2-TPR) was performed to investigate reducibility of the catalysts. The measurement was carried out in a quartz microreactor by using the Micrometrics Chemisorbs 2750 automated system. First, the sample (100 mg) was pretreated in Ar (99.99%, 30 mL/min) at 200 °C for 1 h, and then cooled down to room temperature. After cooling to room temperature in Ar, it was followed by a temperature-programmed reduction by 10% H_2 in Ar (30 mL/min) from room temperature to 850 °C with a temperature ramp of 10 °C/min. Hydrogen consumption was monitored by a thermal conductivity detector (TCD).

H_2-chemisorption (H_2-TPD) was performed to investigate reducibility of the catalysts. The measurement was carried out in a quartz microreactor by using the Micrometrics Chemisorbs 2750 automated system. First, the sample (100 mg) was pretreated in Ar (99.99%, 30 mL/min) at 200 °C for 1 h, and then cooled down to room temperature. After cooling to room temperature in Ar, it was followed by a temperature-programmed reduction by 5% H_2 in Ar (30 mL/min) from room temperature to 480 °C with a temperature ramp of 10 °C/min for 2 h then cooling to room temperature. Last, turned to Ar (99.99%, 30 mL/min) for 30 min, then converted to 10% H_2 in Ar (30 mL/min), followed heating by a temperature-programmed from room temperature to 1000 °C with a temperature ramp of 10 °C/min Hydrogen chemisorption was monitored by a thermal conductivity detector (TCD).

Near Ambient Pressure X-ray Photoelectron Spectroscopy (NAP-XPS) was performed to determine the surface composition and oxidation state of Sn and W on the catalyst. XPS data was collected on a Thermo ESCALAB 250XI XPS system equipped with a monochromatic Al X-ray source operating at 10 mA and 15 kV (energy resolution ~0.5 eV). Regional Sn 3d and W 4f scans were acquired using 20 sweeps with a dwell time of 60 seconds. Peak fitting was performed using Avantage and XPS peak software. Composition was calculated using built-in relative sensitivity factors (RSF). Procedure: Unreduced samples were placed in a sample tank, passed through Ar at 30 mL/min, held for half an hour, heated from room temperature to 200 ^{o}C at a heating rate of 10 ^{o}C/min, and then reduced to room temperature. Spectra were recorded at room temperature. Replace Ar with 5% H_2/Ar and heat from room temperature to 480 ^{o}C at a rate of 20 ^{o}C/min for 2 hours. Allow to cool naturally. Spectra of samples were collected at 250 ^{o}C during the cooling process.

X-ray photoelectron spectroscopy (XPS) was performed to determine the surface composition and oxidation state of Sn and W on the catalyst. XPS data was collected on a Thermo ESCALAB 250XI XPS system equipped with a monochromatic Al X-ray source operating at 10 mA and 15 kV (energy resolution ~0.5 eV). Regional Sn 3d and W 4f scans were acquired using 20 sweeps with a dwell time of 60 seconds. All binding energies were calibrated to the C 1s peak of adventitious carbon at 284.8 eV. Peak fitting was performed using Avantage and XPS peak software. Composition was calculated using built-in relative sensitivity factors (RSF).

X-ray Absorption Spectroscopy (XANES/EXAFS) All XAS data presented in this

article was collected at the beamlines 1W1B at Beijing Synchrotron Radiation Facility. Spectrum were collected at the W L1-edge and W L3-edge. Data was acquired in transmission mode and fluorescence mode. The catalytic were reduction at 480/800 ^{o}C for 2 h in glove box and glove box with sample powder uniformly applied to the tape. The edges of the tape were then sealed to prevent the sample re-oxidation. For each sample, the energy was calibrated by collecting spectra of W foil. Fits were performed using the Demeter package.

Aberration-corrected high-angle annular dark-field scanning transmission electron microscopy (AC-TEM) (JEOL JEM-ARM200F, 200 kV) and energy-dispersive X-ray spectroscopy (EDS) was conducted on a JEOL double Cs corrected TEM/AC-TEM operated at 200 kV accelerating voltage. Samples were prepared by drop-casting reduced catalyst suspension on ultra-thin carbon coated copper grid.

Inductively coupled plasma mass spectrometry (ICP-MS) The element ratio was detected with Agilent 7800. Pump Rate: 29 r/min. Nebulizer Flow: 0.86 L/min. Auxiliary Gas: 0.7 L/min. Sample Flush Time: 40 s. RF Power: 1300 W.

High temperature Gel Permeation Chromatography (HT-GPC). The plastics were analyzed by the high-temperature gel permeation chromatography (HT-GPC). HT-GPC was performed using Agilent PL-GPC50 and Agilent PL-GPC220. The mobile phase, 1,2,4-trichlorobenzene (HPLC grade; Fisher Chemical).

Column: MIXEDB + 2MIXEDD

Solvent: 1,2,4-trichlorobenzene

Flow rate: 1.00 mL/min

Detector: RI

Temperature: 150 °C

Instrument: Agilent 1260II HT GPC

Pretreatment: Shake PE 160 °C for 1 hour, PP 150 °C for 1 hour, and filter the sample after dissolution.

Supplementary Figures and Tables

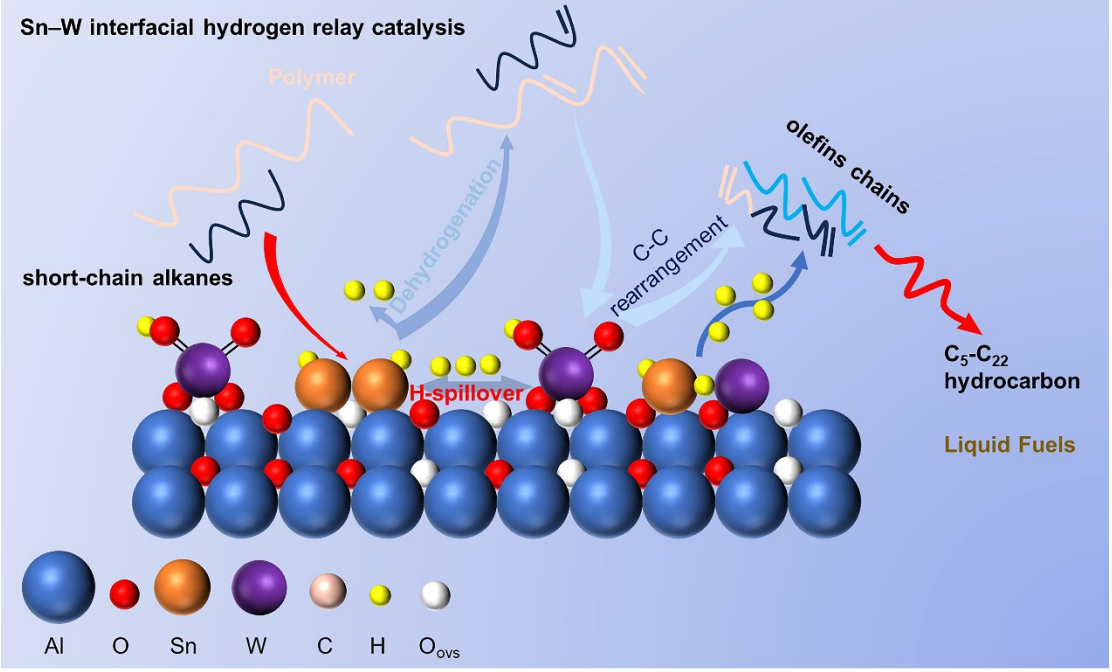

Scheme S1. The mechanism diagram of the catalyst catalyzing the degradation of polyolefin plastics.

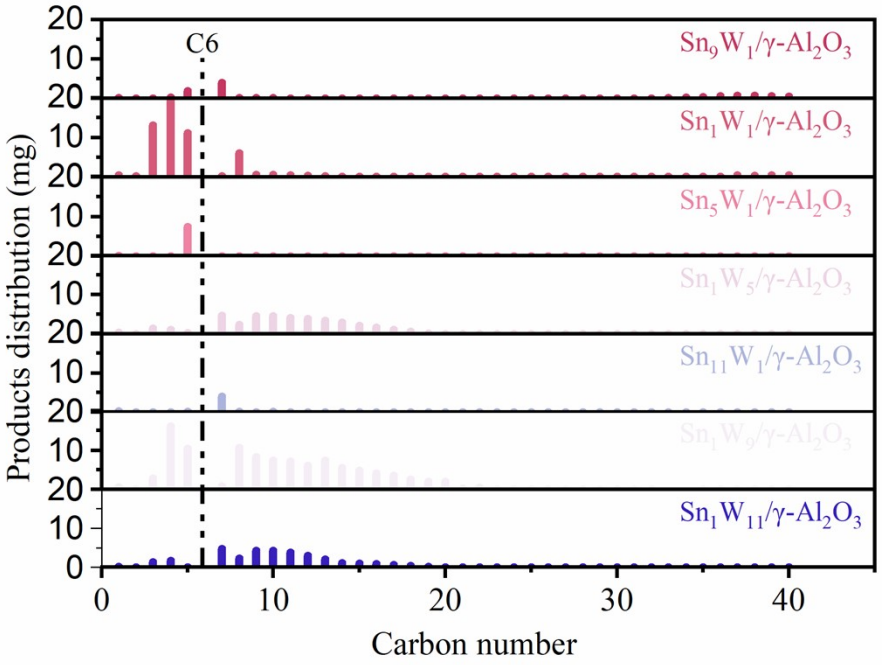

Figure S1. Product distribution of PE degradation catalyzed by different atomic ratios Sn-W catalysts under high solvent-to-plastic ratio (plastic : n-hexane = 1 : 27.3, wt%) conditions. *Reaction:* $Sn_1W_9/\gamma\text{-}Al_2O_3$ (200 mg), PP (120 mg), n-hexane (5 mL), 200 °C, 10 min.

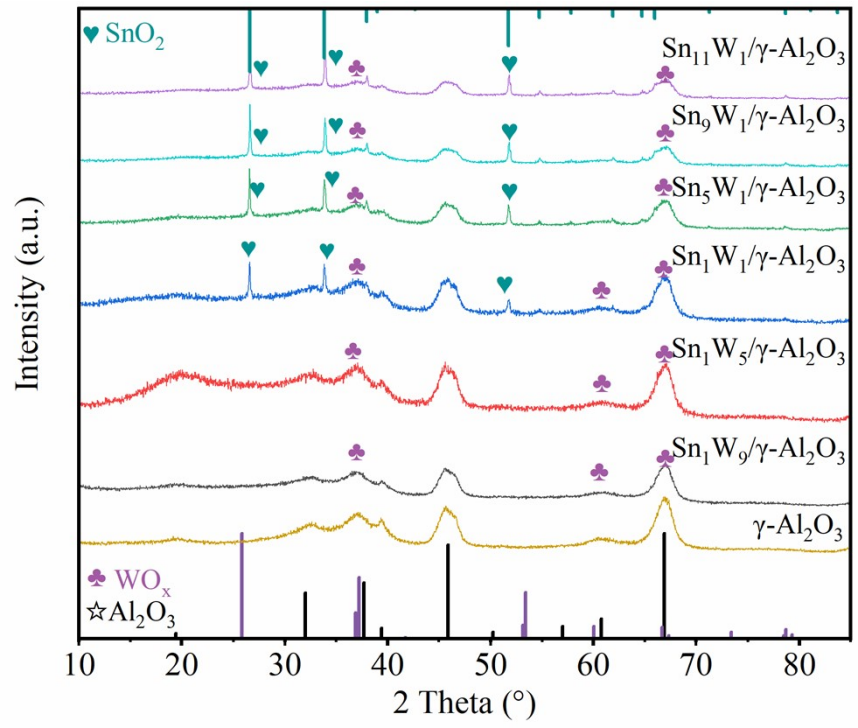

Figure S2. The XRD patterns of Sn-W catalysts with different atomic ratios.

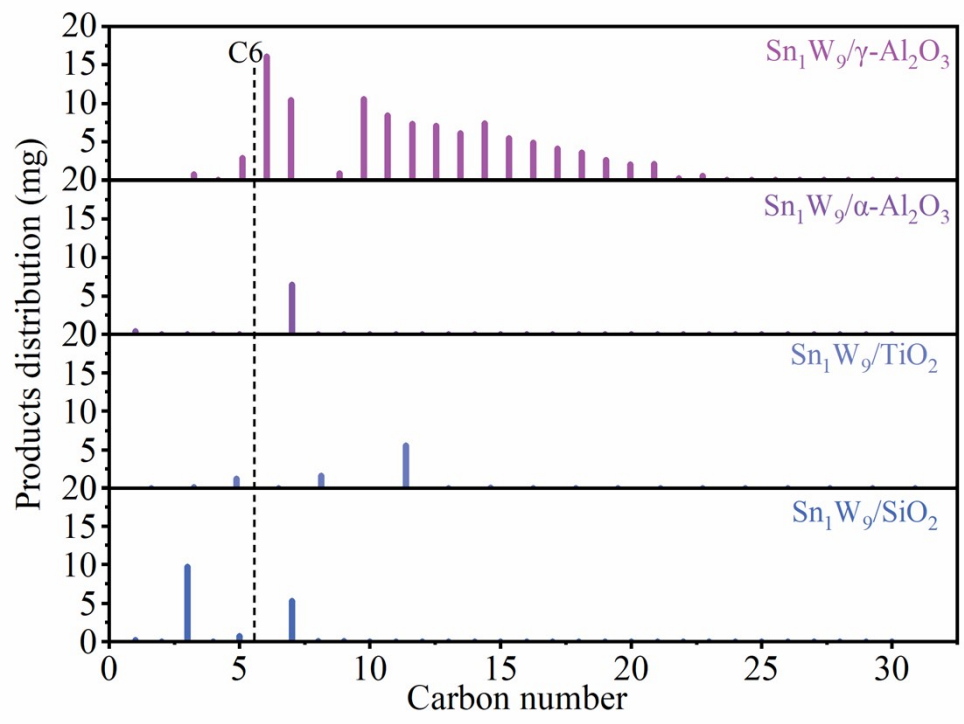

Figure S3. Product distribution of PE degradation catalyzed by Sn-W catalysts with different supports under high solvent-to-plastic ratio (plastic : n-hexane = 1 : 27.3, wt%) conditions. *Reaction:* Sn_1W_9/γ-Al_2O_3 (200 mg), PP (120 mg), n-hexane (5 mL), 200 °C, 10 min.

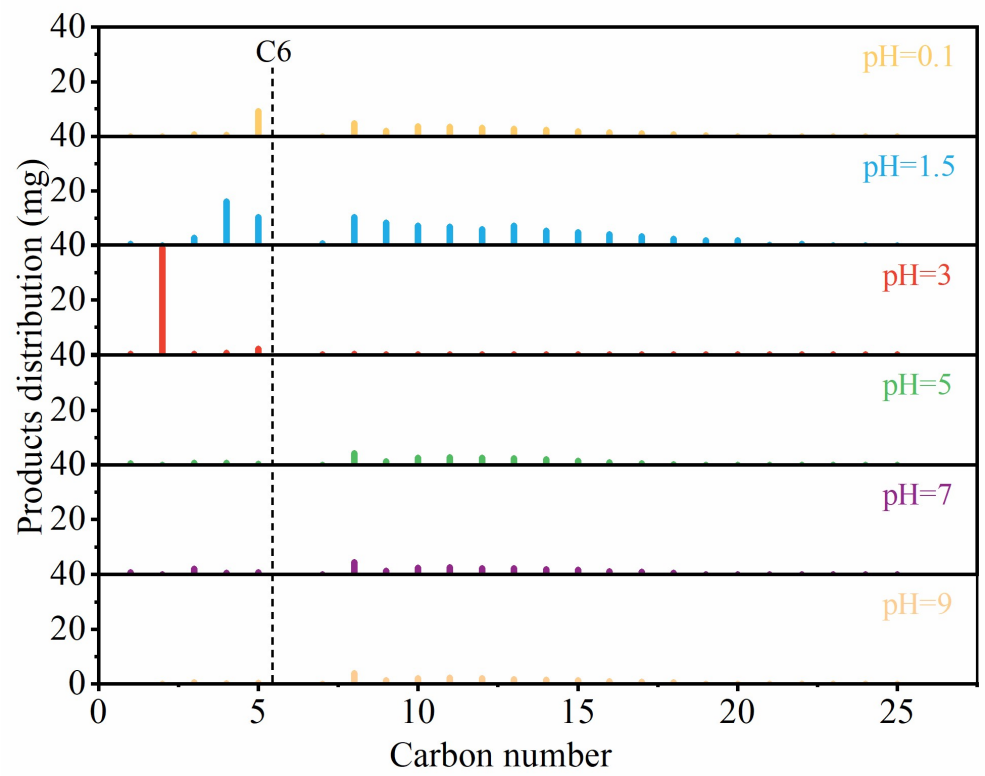

Figure S4. Product distribution of PE degradation catalyzed by Sn-W catalysts with different impregnation pH under high solvent-to-plastic ratio (plastic : n-hexane = 1 : 27.3, wt%) conditions. *Reaction*: $Sn_1W_9/\gamma\text{-}Al_2O_3$ (200 mg), PP (120 mg), n-hexane (5 mL), 200 °C, 10 min.

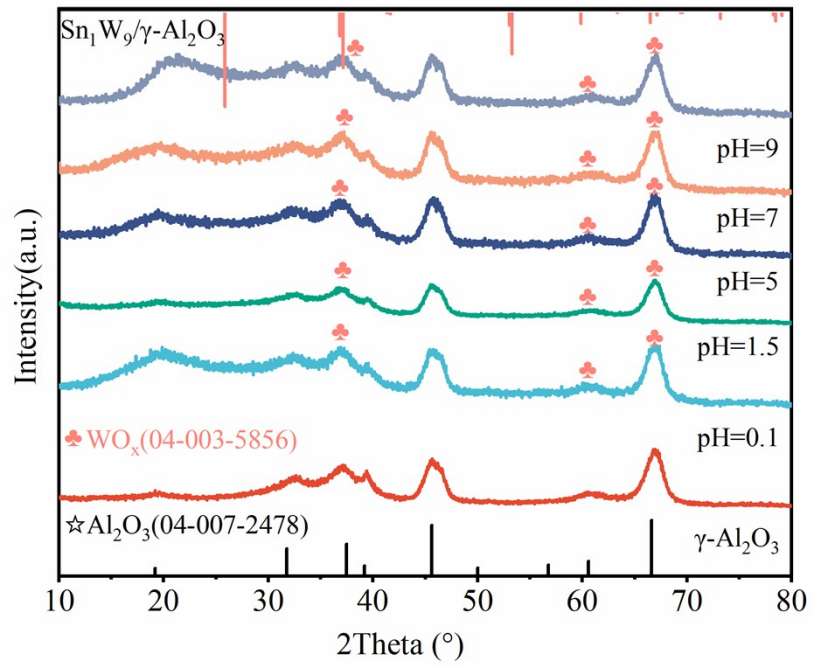

Figure S5. The XRD patterns of Sn-W catalysts with different impregnation pH.

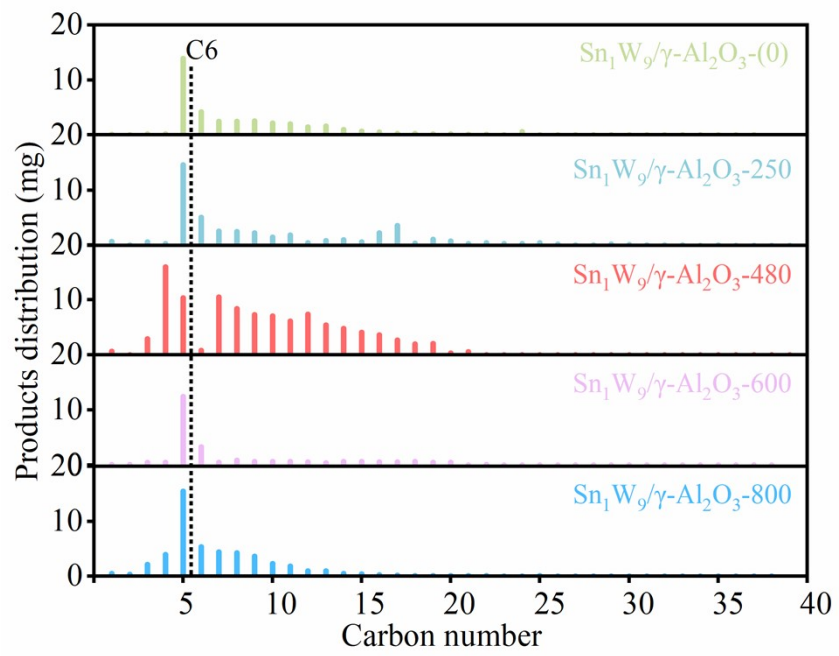

Figure S6. Product distribution of PE degradation catalyzed by Sn-W catalysts with different reduction temperature under high solvent-to-plastic ratio (plastic : n-hexane = 1 : 27.3, wt%) conditions. *Reaction:* $Sn_1W_9/\gamma\text{-}Al_2O_3$ (200 mg), PP (120 mg), n-hexane (5 mL), 200 °C, 10 min.

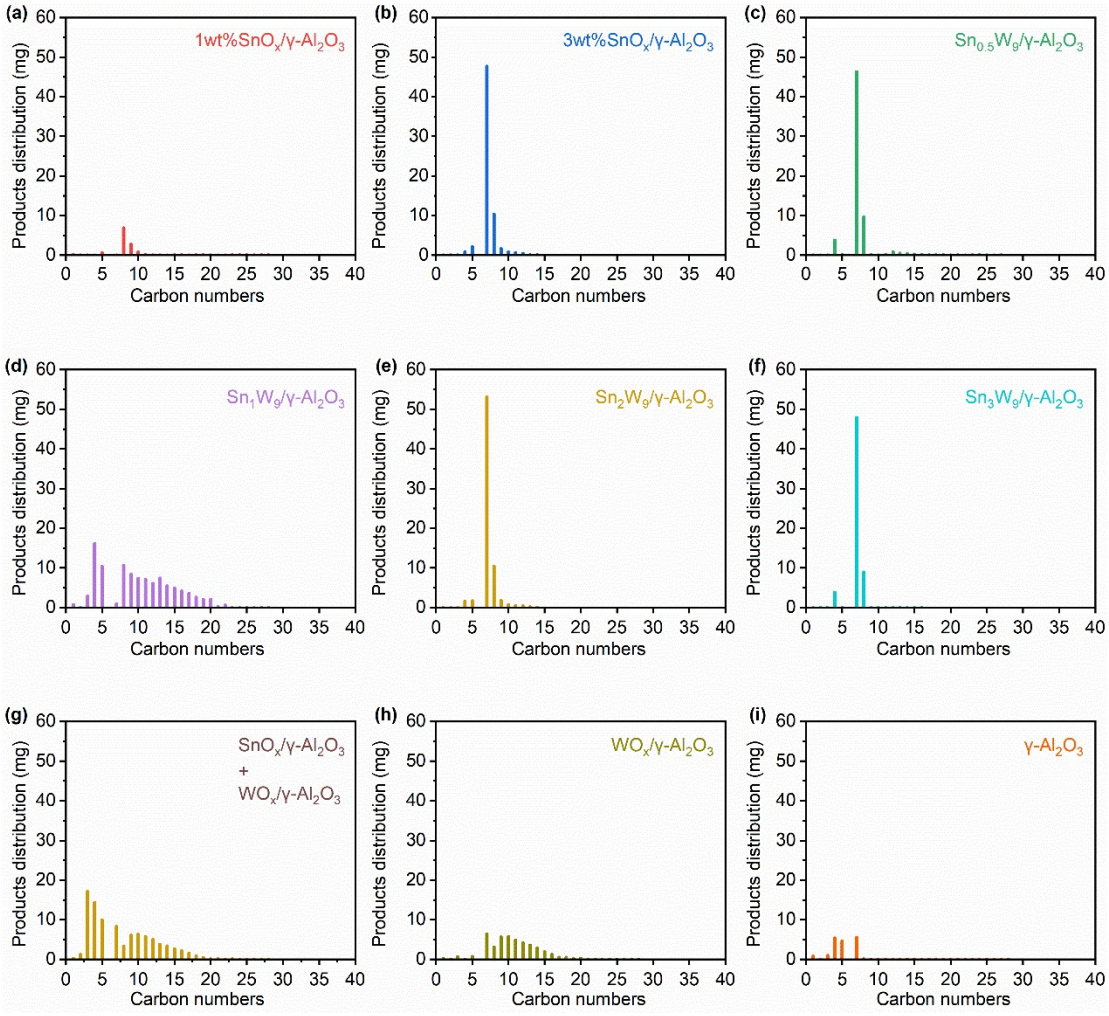

Figure S7. Product distribution of PE degradation catalyzed by $Sn_1W_9/\gamma\text{-}Al_2O_3$ catalyst and control catalyst catalyzed experiments under high solvent-to-plastic ratio (plastic : n-hexane = 1 : 27.3, wt%) conditions. *Reaction:* Catalyst (200 mg), PP (120 mg), n-hexane (5 mL), 200 °C, 10 min.

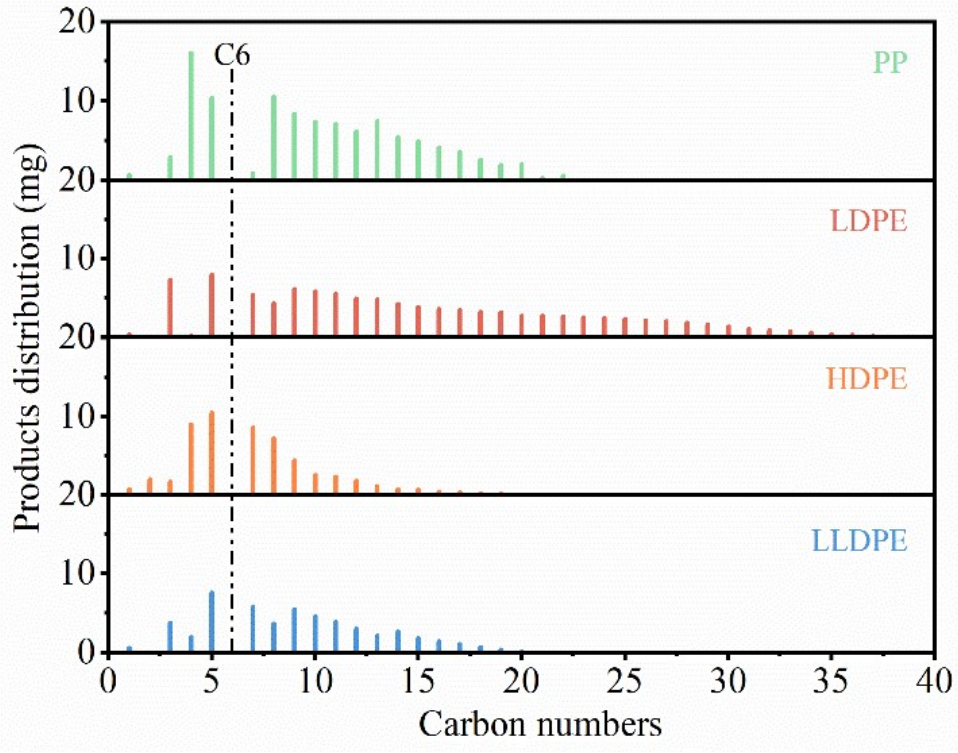

Figure S8. Product distribution of PE degradation catalyzed by $Sn_1W_9/\gamma\text{-}Al_2O_3$ catalyst under high solvent-to-plastic ratio (plastic : n-hexane = 1 : 27.3, wt%) conditions. *Reaction:* $Sn_1W_9/\gamma\text{-}Al_2O_3$ (200 mg), PP (120 mg), n-hexane (5 mL), 200 °C.

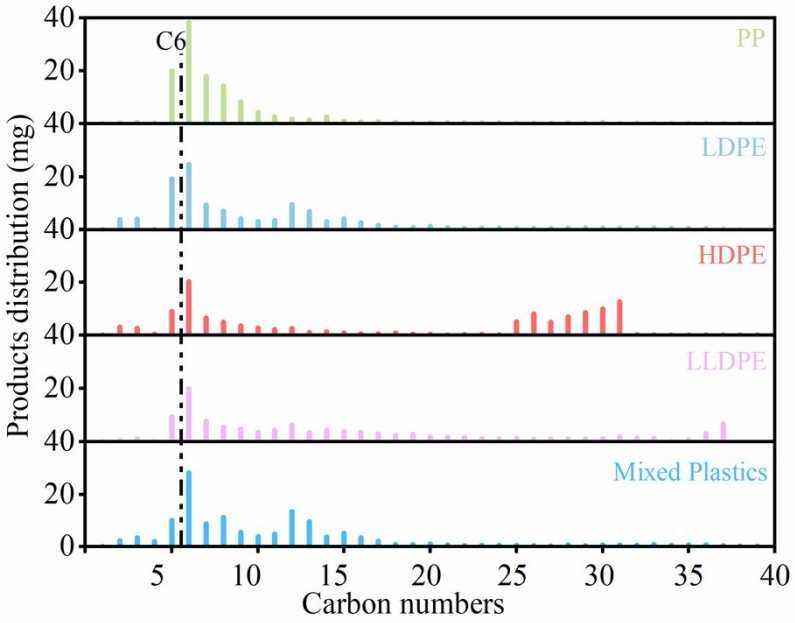

Figure S9. Product distribution of PE degradation catalyzed by $Sn_1W_9/\gamma\text{-}Al_2O_3$ catalyst under low solvent-to-plastic ratio (plastic : n-hexane = 1 : 5, wt%) conditions. *Reaction*: $Sn_1W_9/\gamma\text{-}Al_2O_3$ (200 mg), PP (120 mg), n-hexane (910 μL), 250 °C.

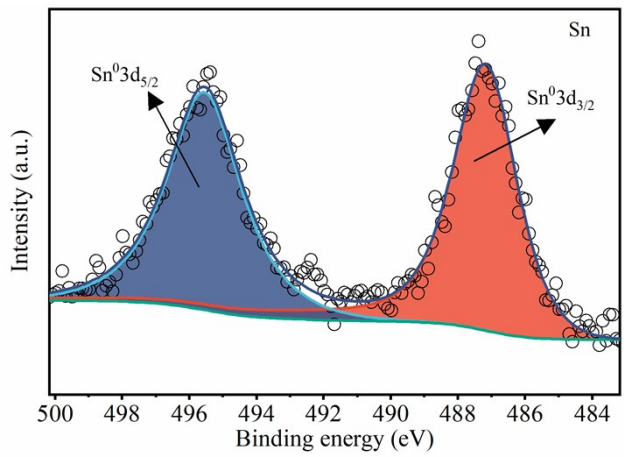

Figure S10. Sn 3d of the XPS spectroscopic spectra of pristine Sn_1W_9/γ-Al_2O_3-(480) measured by NAP-XPS at 250 ^oC.

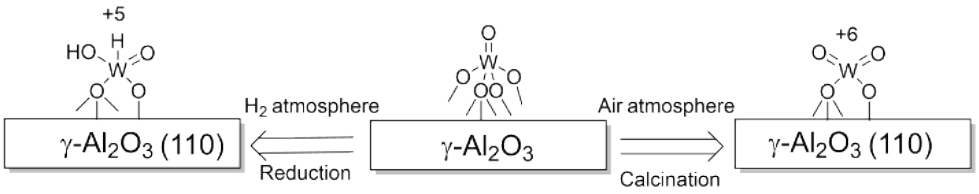

Figure S11. Structural evolution of WO_x species supported on γ-Al_2O_3 under calcination in air and subsequent high-temperature treatment in H_2/Ar atmosphere.

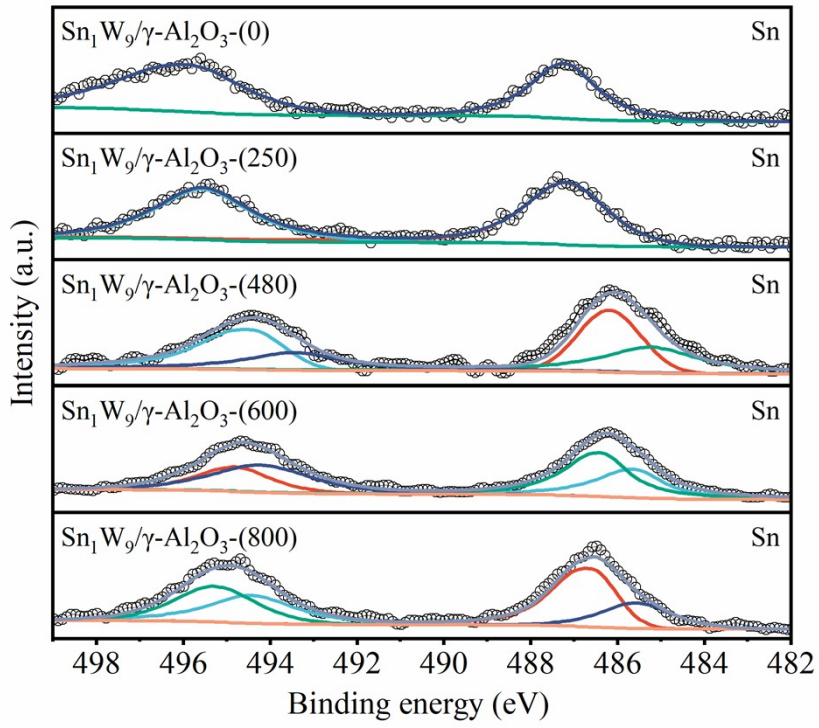

Figure S12. XPS of Sn 3d of $Sn_1W_9/\gamma\text{-}Al_2O_3$-(0, 250, 480, 600, 800 ^oC) catalysts.

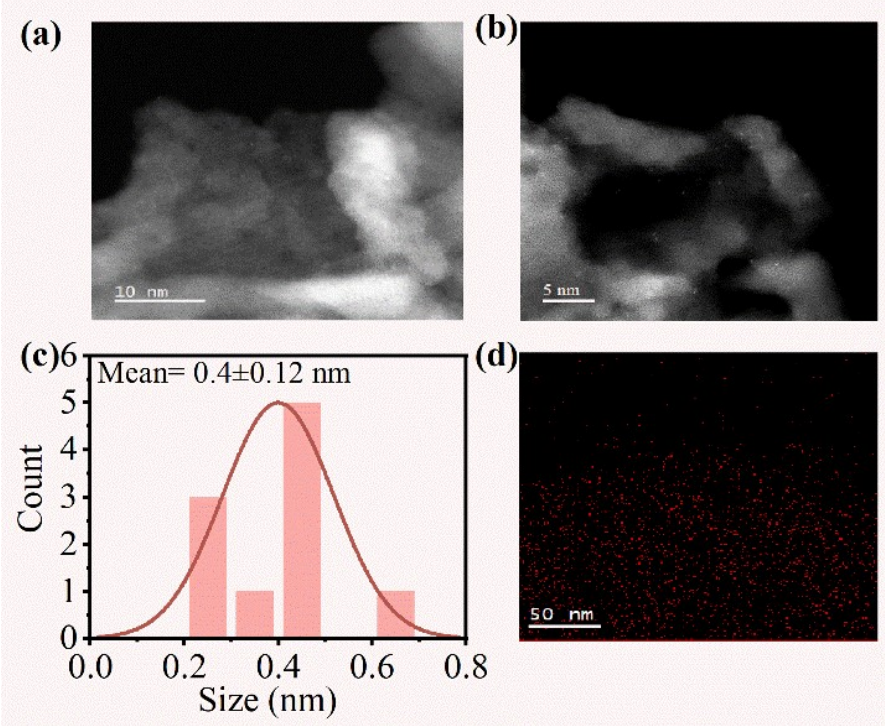

Figure S13. Characterizations of SnO_x/γ-Al_2O_3. (a-b) HAADF-STEM image of SnO_x/γ-Al_2O_3 (10 nm, 5 nm). (c) Particle size scale distribution statistics and cumulative frequency distribution statistics of SnO_x/γ-Al_2O_3. (d) EDS mapping images of SnO_x/γ-Al_2O_3 (deep red: Sn element).

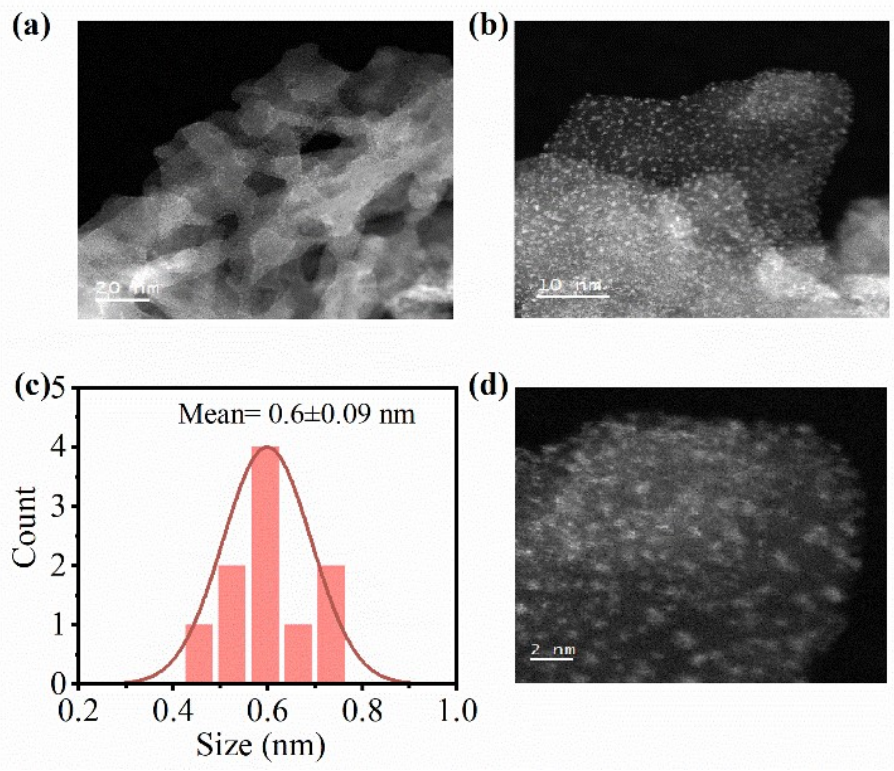

Figure S14. Characterizations of WO_x/γ-Al_2O_3. (a, b, d) HAADF-STEM image of WO_x/γ-Al_2O_3 (20 nm, 10 nm, 2 nm). (c) Particle size scale distribution statistics and cumulative frequency distribution statistics of WO_x/γ-Al_2O_3.

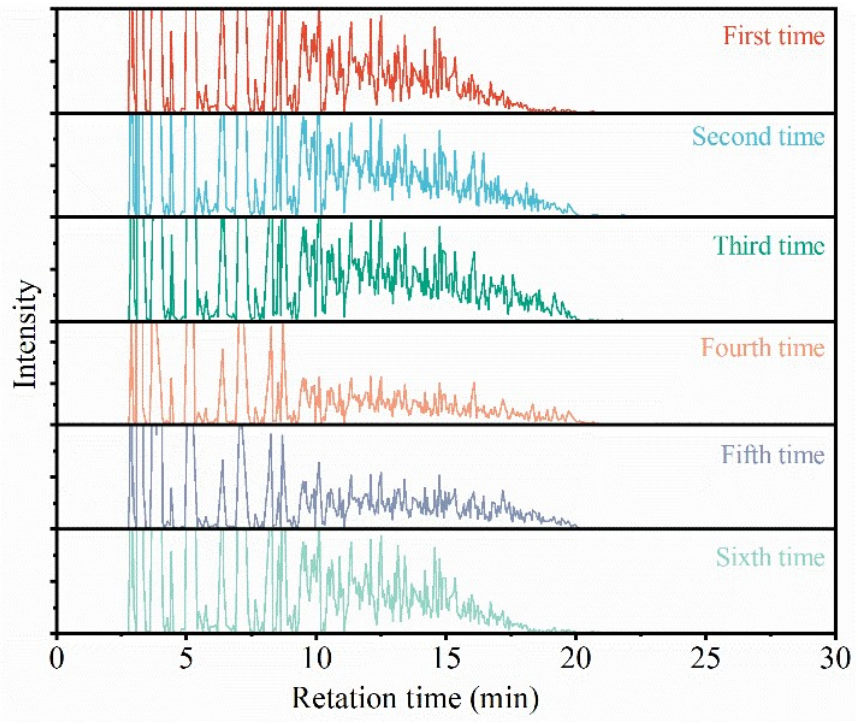

Figure S15. The products distributions of which under low solvent/plastic ratio catalytic degradation of PP plastics using $Sn_1W_9/\gamma\text{-}Al_2O_3$ catalyst for at least five cycle experiments.

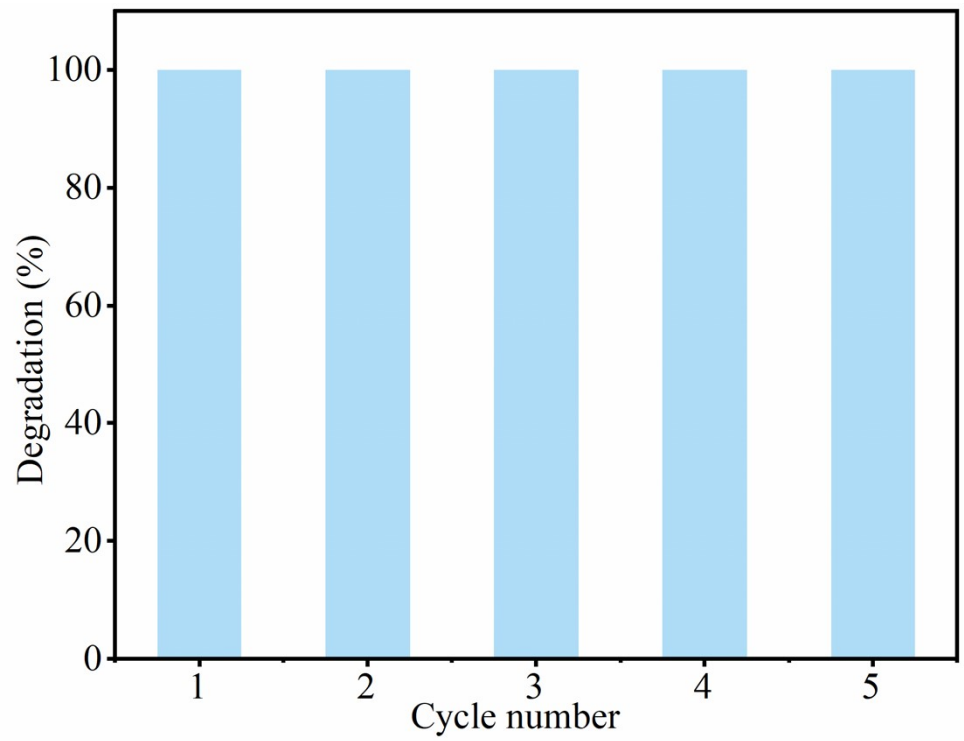

Figure S16. The activity of Sn_1W_9/γ-Al_2O_3 catalyst for at least five cycles which under low solvent/plastic ratio catalytic degradation of PP plastics.

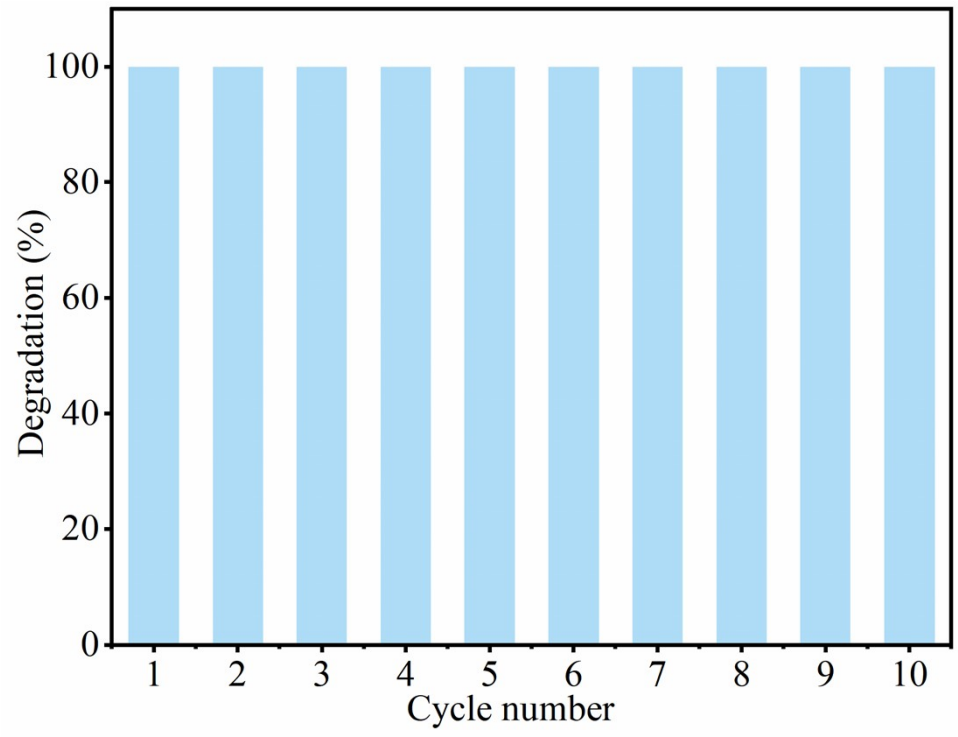

Figure S17. Catalyst stability evaluation over 10 successive cycles. *Reaction:* Sn_1W_9/γ-Al_2O_3 (200 mg), PP (120 mg), n-hexane (5 mL), 200 °C, 10 min.

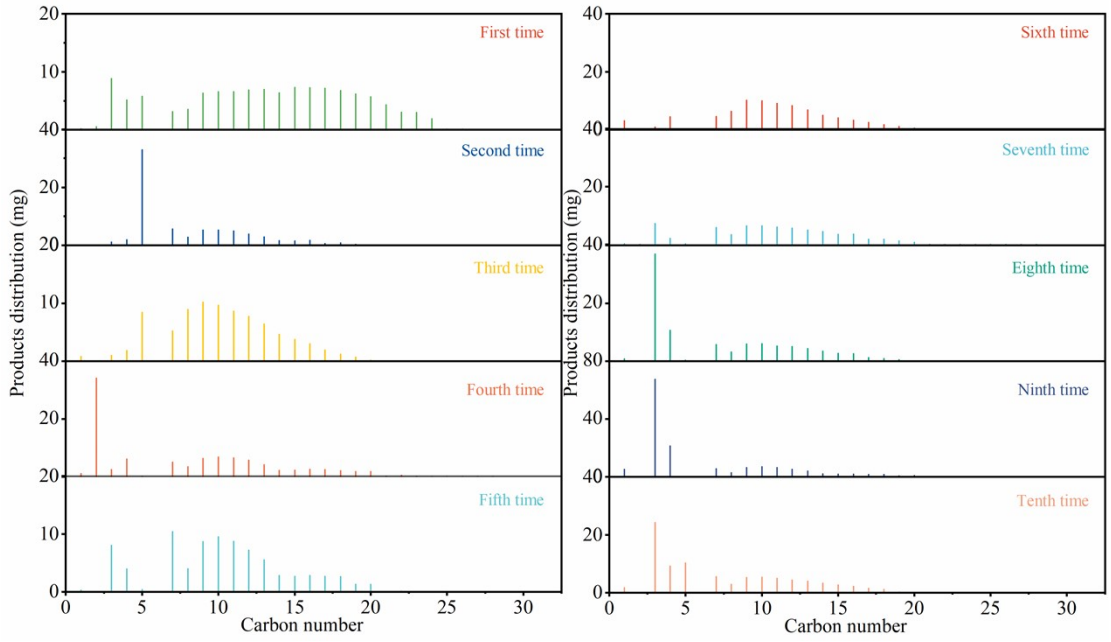

Figure S18. Distribution of products in stability tests of the $Sn_1W_9/\gamma\text{-}Al_2O_3$ catalyst.

Reaction: $Sn_1W_9/\gamma\text{-}Al_2O_3$ (200 mg), Plastics (120 mg), n-hexane (5 mL), 200 °C, 10 min.

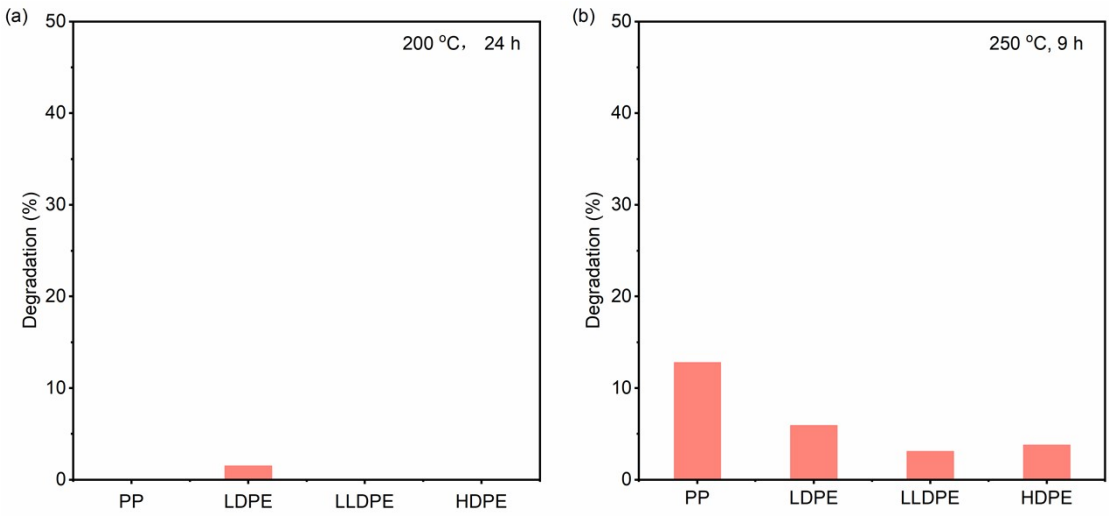

Figure S19. (a) Degradation rate of polyolefin plastic under high solvent-to-plastic mass ratio conditions. (b) Degradation rate of polyolefin plastic under low solvent-to-plastic mass ratio conditions.

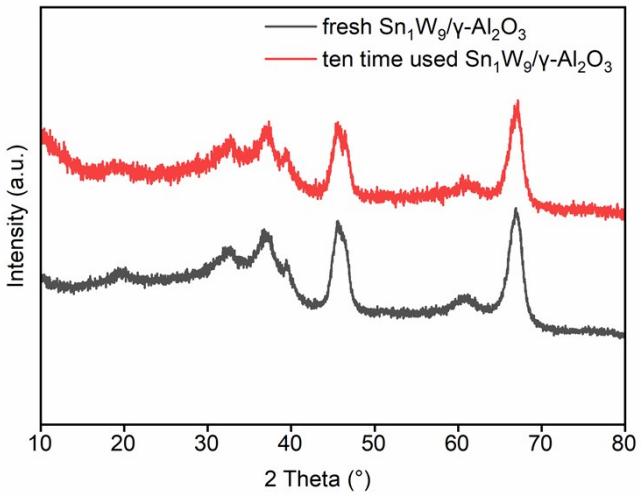

Figure S20. XRD patterns of the catalyst before and after ten catalytic cycles.

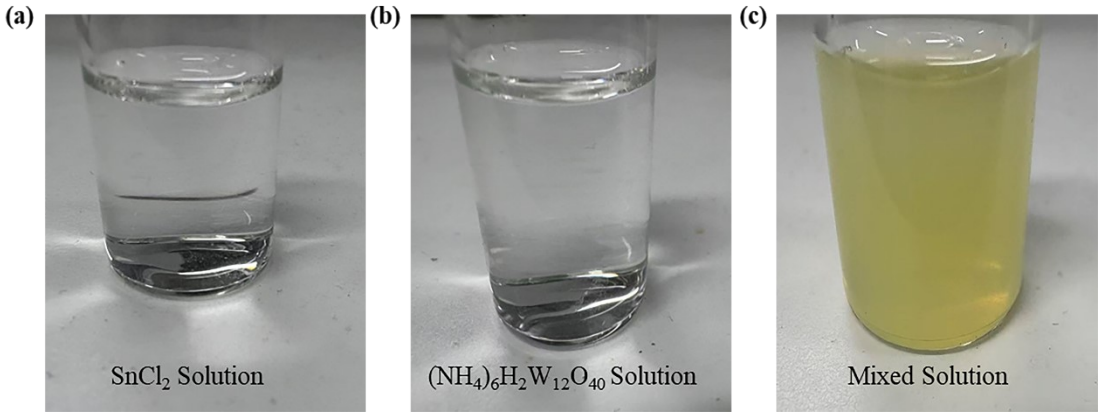

Figure S21 (a) The color of $SnCl_2$ when dissolved in an HCl solution with a pH of 1.55. b) The color of $(NH_4)_6H_2W_{12}O_{40}$ when dissolved in an HCl solution with a pH of 1.55. (c) The color of a mixture of $SnCl_2$ and $(NH_4)_6H_2W_{12}O_{40}$ when dissolved in an HCl solution with a pH of 1.55.

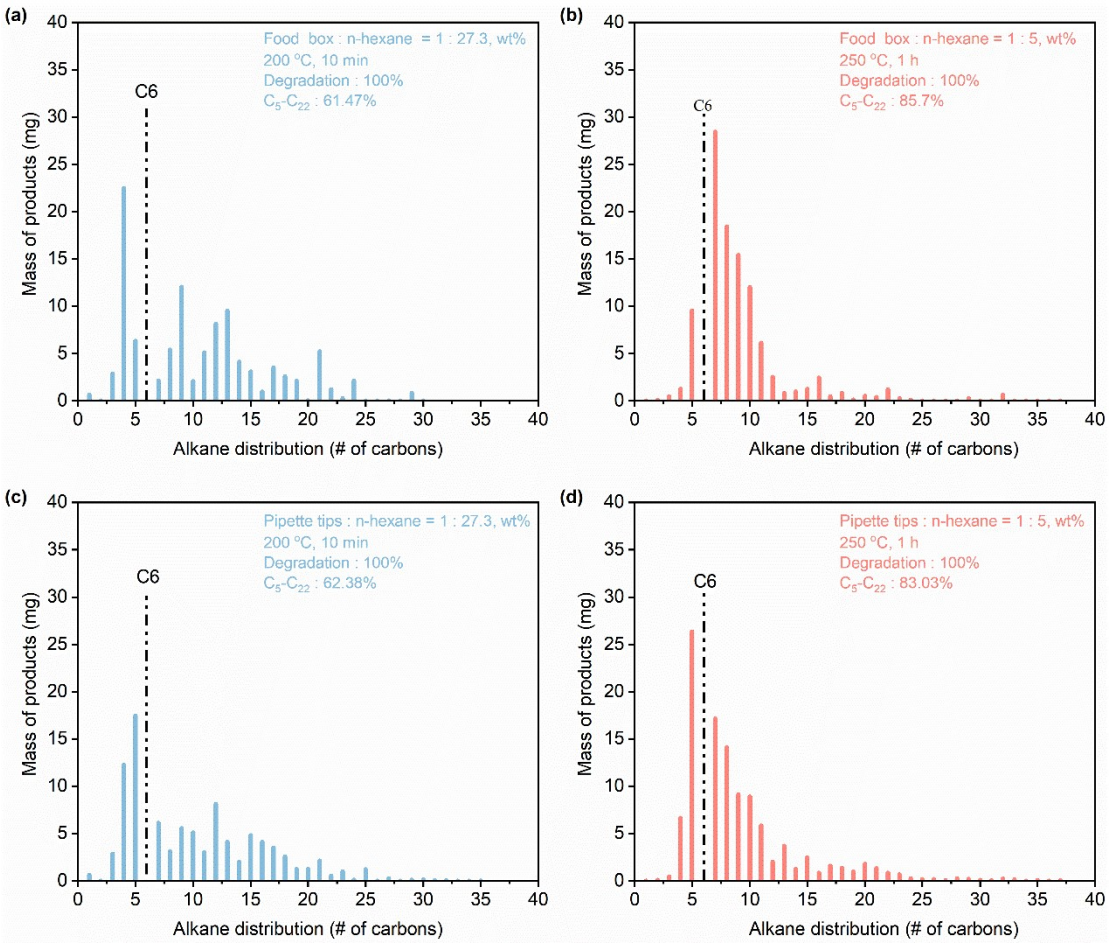

Figure S22. Product distribution of Food box/Pipette tips degradation catalyzed by $Sn_1W_9/\gamma\text{-}Al_2O_3$ catalyst under high (a, c) and low (b, d) solvent-to-plastic ratios. High ratio: plastic : n-hexane = 1 : 27.3, 200 °C, 10 min; Low ratio: plastic : n-hexane = 1 : 5, 250 °C, 1 h.

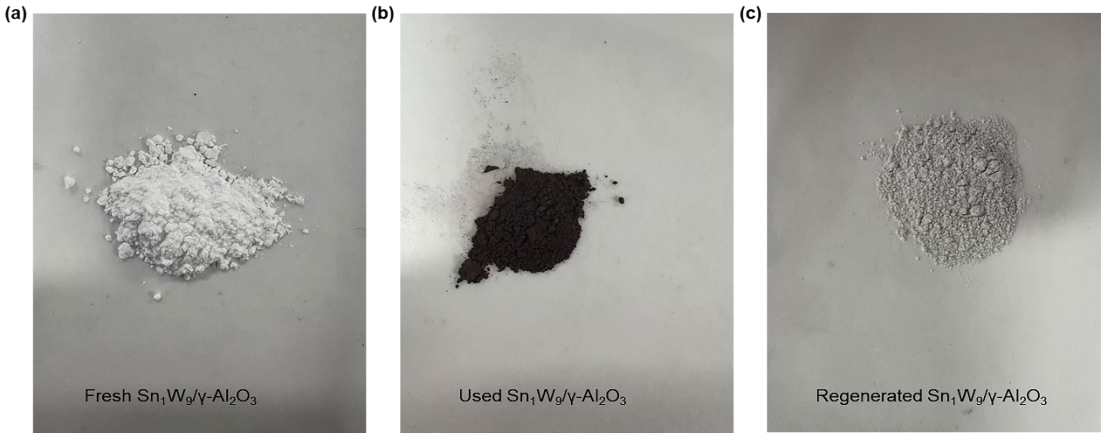

Figure S23 (a) The color of fresh Sn_1W_9/γ-Al_2O_3 catalyst. (b) The color of used Sn_1W_9/γ-Al_2O_3 catalyst. (c) The color of regenerated Sn_1W_9/γ-Al_2O_3 catalyst.

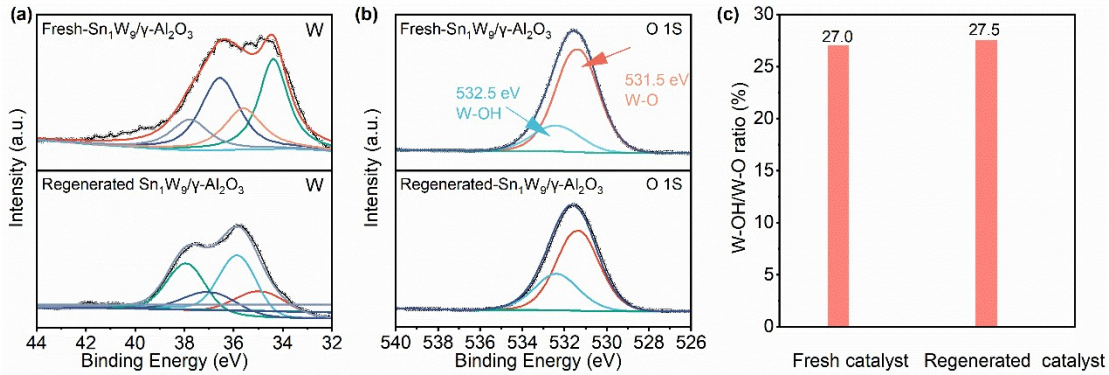

Figure S24 (a) W 4f NAP-XPS spectra of Fresh $Sn_1W_9/\gamma\text{-}Al_2O_3$ and Regenerated $Sn_1W_9/\gamma\text{-}Al_2O_3$ catalyst. (b) O 1s NAP-XPS spectra of Fresh $Sn_1W_9/\gamma\text{-}Al_2O_3$ and Regenerated $Sn_1W_9/\gamma\text{-}Al_2O_3$ catalyst, highlighting the lattice oxygen (W–O) and surface hydroxyl (W–OH) components. (c) Deconvoluted O 1s spectra of Fresh $Sn_1W_9/\gamma\text{-}Al_2O_3$ and Regenerated $Sn_1W_9/\gamma\text{-}Al_2O_3$ catalyst, showing the integrated area ratio of W–OH to W–O species.

Table S1. The Sn-W elemental ratio of Sn_1W_9/γ-Al_2O_3 from High-resolution Transmission Electron Microscopy.

Entry	Element	Atomic Fraction (%)
1	Sn	10.42
2	W	89.58

Table S2. The ICP-MS of $Sn_1W_9/\gamma\text{-}Al_2O_3$.

Entry	Element	Element content (wt.%)	Sn/W Ratio
1	Sn	0.77	1:13
2	W	10.21	

Table S3. Comparison of catalytic results for the chemical upgrading of PE via alkane metathesis in recent literature, highlighting solvent-to-polymer mass ratio, gasoline/diesel selectivity (C_5-C_{22}, excluding C_6), and degradation efficiency.

Catalyst	Plastics	Conditions	Solvent / PE ratio (g/g)	Selectivity (C_5-C_{22})	Yield (%)
Sn_1W_9/γ-Al_2O_3 (200 mg)	PP (120 mg) Mw=82.0 KDa	250 °C, 1 h	5	95%	100
[Ir-H], Re_2O_7/γ-Al_2O_3	PE (120 mg) Mw=3.35 KDa	175 °C, 96 h	14.6	85%	100
SnPt/γ-Al_2O_3 (500 mg) Re_2O_7/γ-Al_2O_3 (500 mg)	PE (250mg) Mw=54.1 KDa	200 °C, 15 h	20	39%	73
WO_x/SiO_2 (0.8 g) Zeolite 4 A (1 g)	LDPE (1.6g) Mw=75.0 KDa	300 °C, 2 h, 30 bar N_2	6.3	65.5%	75

Table S4. Cross metathesis of PP (120 mg) with n-hexane (5 mL) using $Sn_1W_9/\gamma\text{-}Al_2O_3$ catalyst: The conversion of PP to oil and wax products and the distribution of soluble n-alkane products after heating the mixture for 10 min at 200 °C. The amounts of soluble products were determined by GC analysis with C_7-C_{40} in n-hexane (1000 μg/mL) as an external standard. The gas products were determined by GC analysis with CO_2 as an internal standard.

Catalyst	PE_S (mg)	n-hexane (mg)	Temperature (°C)	Time (h)	C_3-C_{30} (mg)	Mass ratio (%)
$Sn_1W_9/\gamma\text{-}Al_2O_3$	0	3300	200	0.17	8.95	0.27
$Sn_1W_9/\gamma\text{-}Al_2O_3$	0	3300	250	9	16.32	0.5
$Sn_1W_9/\gamma\text{-}Al_2O_3$	0	3300	250	48	17.5	0.53
1#-Ir-H $Re_2O_7/\gamma\text{-}Al_2O_3$	0	1980	150	72	1219.7	61.6
2#-Ir-H $Re_2O_7/\gamma\text{-}Al_2O_3$	0	1980	150	72	913	46.1

Table S5. Py-IR characterization of $Sn_1W_9/\gamma\text{-}Al_2O_3$ catalysts, total acid amount, B acid amount and L acid amount.

Temperature (°C)	B acid area ($cm^{-1}\cdot mg^{-1}$)	L acid area ($cm^{-1}\cdot mg^{-1}$)	B acid volume (μmol/g)	L acid volume (μmol/g)	B/L ratio
200	0.229	1.67	9.280	51.118	0.181
350	0.132	0.88	5.349	26.936	0.198

Table S6. GPC testing of different types of polyolefin plastics and different types of commercial plastics.

Polymer	Mn(kDa)	Mw(kDa)	PDI
PP	32.5	82.6	2.5
LDPE	41.1	161.9	3.9
LLDPE	32.3	131.2	4.1
HDPE	44.7	127.7	2.8
Food box	46.8	113.9	2.4
Melt blown	42.1	95.9	2.3
Pipette tips	38.7	200.0	5.1
Drug bottles	55.6	219.6	3.9
Dove bottles	22.2	125.3	5.6
Packing bags	34.3	91.4	2.7

Table S7. Life Cycle Analysis (LCA) Evaluation of Sn-W/γ-Al_2O_3 Catalyst and a benchmark catalyst.

Catalyst	Temp. (°C)	Time (h)	GWP_m (KJ)	$E_{Reaction}$ (MJ)	Total GWP (Renew.)	Total GWP (Fossil)
Sn–W/γ-Al_2O_3 (This work)	250	1	2.11	8.3	2.53	5.85
$SnPt/Al_2O_3$	200	15.0	5.9	2.5	6.03	7.03
Re_2O_7/Al_2O_3 WO_x/SiO_2	300	2.0	2.1	4.0	2.30	3.90
Zeolite 4A [Ir-H] Re_2O_7/Al_2O_3	175	96.0	7.5	5.5	7.78	9.98
$Pt/SrTiO_3$	300	96	4.3	5.0	4.55	6.55
Ru/CeO_2	240	1.0	2.8	3.0	2.95	4.15
Ru/HZSM-5	280	24.0	3.0	4.0	3.20	4.80
Pt-Fe/Al_2O_3	330	24.0	2.9	3.2	3.06	4.34

The life cycle assessment (LCA) of the catalytic systems for plastic upgrading includes reaction energy consumption, contributions from individual metal components, and the overall carbon footprint. All values were calculated in accordance with ISO 14040/44 standards. To enable direct comparison with other representative catalytic systems (e.g., Ru-, Ir-, and Pt-based catalysts), reaction conditions of 250 °C for 1 h with 120 mg of plastic were selected. To avoid inconsistency with the larger-scale experiments reported in this work (280 °C, 48 h, continuous catalytic degradation of 1364 mg plastic), the functional unit was defined as the treatment of 1 kg of

polypropylene, and all data were normalized accordingly to ensure consistency and robustness of the comparison.

In laboratory-scale experiments, the nominal power of the catalytic reactor (P_0) is typically 1.0 kW at 250 °C. However, the Life Cycle Assessment (LCA) results are normalized to the treatment of 1 kg of plastic, which represents an industrial-scale equivalent. The apparent power discrepancy arises from this normalization process.

- Scaling and Normalization Principle

For laboratory tests:

$E_{exp} = P_0 \times t = 1 \times 1 = 1$ kWh (actual energy consumption)

$m_{exp} = 120$ mg $= 0.00012$ kg

Hence, Et(lab) $= E_{exp} / m_{exp} = 8333$ kWh·kg^{-1}.

However, such a high value does not represent realistic industrial operation. To evaluate sustainable catalytic performance, the LCA framework rescales this energy consumption to a hypothetical industrial system treating 1 kg of plastic under the same temperature and time conditions.

- Reverse Derivation of Equivalent Power

To maintain a normalized reaction energy ($E_t = 8.3$ kWh·kg^{-1}) at t = 1 h for 1 kg of plastic, the equivalent reactor power (P_{eq}) is computed as:

$P_{eq} = (E_t \times m_p) / t = (8.3 \times 1) / 1 = 8.3$ kW

Thus, the 8.3 kW value corresponds to the equivalent industrial-scale reactor power required to process 1 kg of plastic within 1 h, yielding an energy intensity of 8.3 kWh·kg^{-1}.

- LCA evaluation follows the equations below:

- $E_t = (P \times t) / m_p$ — Reaction energy consumption (kWh·kg^{-1})

- $GWP_m = \Sigma(L_i / 100 \times EF_i)$ — Metal carbon footprint (kg CO_2 e·kg^{-1})
- $GWP_e = E_t \times EF_{ele}c$ — Electricity-related emission (kg CO_2 e·kg^{-1})
- $GWP_{total} = GWP_m + GWP_e$ — Total life-cycle carbon footprint

Here, P is the reactor power (kW), t is reaction time (h), m_p is mass of plastic (kg), L_i is metal loading (wt%), EF_i is emission factor (kg CO_2 e·kg^{-1} metal), and $EF_{ele}c$ represents the electricity emission factor (0.05 for renewable and 0.45 for fossil electricity).

➢ Example: Sn_1W_9/γ-Al_2O_3 Catalyst

Given: P = 8.3 kW, t = 1 h, m_p = 1 kg, L(Sn) = 0.77 wt%, L(W) = 10.21 wt%.

Step 1. Reaction energy consumption: $E_t = (8.3 \times 1) / 1 = 8.3$ kWh·kg^{-1}

Step 2. Metal carbon footprint: $GWP_m = 0.0077 \times 4.8 + 0.1021 \times 20.3 = 2.11$ kg CO_2 e·kg^{-1}

Step 3. Electricity emissions: GWP_e (renewable) = 8.3×0.05 = 0.42; GWP_e (fossil) = 8.3×0.45 = 3.74

Step 4. Total emissions: GWP_{total}(renew.) = 2.11 + 0.42 = 2.53; GWP_{total}(fossil) = 2.11 + 3.74 = 5.85

All LCA data were calculated under ISO 14040/44 framework and cross-validated by internal reproducibility checks.

Based on the expanded and normalized dataset, the Sn_1W_9/γ-Al_2O_3 catalyst exhibits the lowest total life-cycle carbon footprint among the benchmarked systems, with a total GWP of 2.53 kg CO_2 e·kg^{-1} (renewable electricity) and 5.85 kg CO_2 e·kg^{-1} (fossil electricity). This value is approximately 50–70% lower than those of representative Pt, Ir, and Re catalysts reported in the literature.

REFERENCE:

1. H. Zhou, Z. Chen, F. Kong, Z. Dou, J. Hu, M. Wang. *Angew. Chem. Int. Ed.,* 2025, **64**, e202516021.

2. C. Wang, T. Xie, P. A. Kots, B. C. Vance, K. Yu, P. Kumar, et al., *JACS Au* 2021, **1**, 1422-1434.

3. J. Fu, S. Liu, W. Zheng, R. Huang, C. Wang, A. Lawal, et al., *Nat. Catal.* 2022, **5**, 144-153.

4. G. Zuo, Y. Xu, J. Zheng, F. Jiang and X. Liu, *RSC Adv.,* 2018, **8**, 8372-8384.

5. Ro, I., Qi, J., Lee, S.*et al., Nature* 2022, **609**, 287–292.

6. S. Lwin, Y. Li, A. I. Frenkel and I. E. Wachs, *ACS Catal.,* 2016, **6**, 3061-3071.

7. Jia, X.; Qin, C.; Friedberger, T.; Guan, Z.; Huang, Z., *Sci. Adv.,* 2016; **2**: e1501591.

8. Chen, Z.; Gong, W.; Wang, J.; Hou, S.; Yang, G.; Zhu, C.; Fan, X.; Li, Y.; Gao, R.; Cui, Y., *Nat. Commun.,* 2023, **14**, 5363.

9. J. G. Howell, Y.-P. Li and A. T. Bell, *ACS Catal.,* 2016, **6**, 7728−7738.

10. G. Celik, R. M. Kennedy, R. A. Hackler, M. Ferrandon, A. Tennakoon, S. Patnaik, et al., *ACS Cent. Sci.*, 2019, **5**, 1795-1803.

11. L. D. Ellis, S. V. Orski, G. A. Kenlaw, A. G. Norman, K. L. Beers, Y. Román-Leshkov, et al., *ACS Sustain. Chem. Eng.,* 2021, **9**, 623-628.

12. Y. Nakaji, M. Tamura, S. Miyaoka, S. Kumagai, M. Tanji, Y. Nakagawa, et al.,

Appl. Catal. B, 2021, **285**, 119805.

13. W. R. Leow, Y. Lum, A. Ozden, Y. Wang, D.-H. Nam, B. Chen, et al., *Science* 2020, **368**, 1228-1233.

14. H. Zhou, Y. Ren, Z. Li, M. Xu, Y. Wang, R. Ge, *et al., Nat. Commun.*, 2021, **12**, 4679.

15. H. Li, J. Wu, Z. Jiang, J. Ma, V. M. Zavala, C. R. Landis, *et al., Science* 2023, **381**, 660-666.

16. Wang, M., Gao, Y., Yuan, S. *et al., Nat. Chem. Eng.,* 2024, **1**, 376–384.

17. U. S. Chaudhari, A. T. Johnson, B. K. Reck, R. M. Handler, V. S. Thompson, D. S. Hartley, et al., *ACS Sustain. Chem. Eng.,* 2022, **10**, 13145–13155.

18. S. Ügdüler, KM. Geem, M. Roosen, et al., *Waste Manag.* 2020, **104**,148-182.